

ASSESSING THE IMPACT OF EXPLOSIONS ON NUCLEAR POWER PLANTS

Waleed Abdel-Latif Attia¹, Basma. M. F. Hassan²

¹ Professor of Structure analysis and mechanics, Department of Structural Engineering, Faculty of Engineering, Cairo University, Egypt.

² Civil engineer, Directors Housing and Utilities, Aswan, Egypt

ABSTRACT

Nuclear power offers a low-carbon energy alternative to fossil fuels, but requires careful management due to its complexity and potential risks. It doesn't produce air pollution or CO2 emissions during operation, making it attractive for countries seeking clean energy sources [1,2]. Many nations throughout the world support nuclear energy as a clean energy source that aligns with the environmental protection idea of "carbon emission reduction." While the European Commission has already appointed nuclear power as a "green" investment, the UK government is currently trying to reclassify nuclear power as "environmentally sustainable" to draw in private investment [2, 3].

For the El-Dabaa Nuclear Power Plant (DNPP), the first of its kind in Egypt, my research focused on the critical role of the reinforced concrete (RC) containment system. This vital barrier acts as the last line of defense, preventing the release of radioactive materials during accidents like earthquakes, fires, explosions, or even terrorist attacks. To assess the response of this containment structure to internal or external explosions, this paper utilized advanced modeling techniques. This analysis involved simulating the generation, propagation, and impact of the blast wave on the structure. Using ANSYS software, this research investigated four scenarios with explosions occurring at varying distances 14.80 meters, 10 meters and 1 meter from the containment. My study revealed a significant influence of material properties, structural dimensions, and the characteristics of the blast itself on the behavior of the containment under extreme loads. Importantly, the findings demonstrate that explosions can cause substantial damage. This information is crucial for the design of even more robust nuclear facilities and the development of advanced repair strategies for structures potentially impacted by blasts.

Keywords: Reinforced concrete containment, Egypt nuclear plant (EL-DABAA), VVER-1200, Blast load, Numerical simulation, Risk assessment

1. Introduction

Nuclear power offers a low-carbon electricity source, but safety remains paramount. Strongly built containment structures, often made of RC, are vital for protecting the environment and public from radiation in case of an accident. These containment shells require careful design and study due to their critical role in nuclear energy production [4, 5, 6, 7]. Nuclear power plants require critical structures to handle extreme dynamic forces. These include internal events (jet forces, pipe ruptures) and external threats (earthquakes, explosions, plane crashes) [8]. Stangenberg's research focuses on calculating the maximum dynamic load capacity of RC beams and plates. His method considers the effects of shear and rotational inertia, acknowledging limitations in wave propagation. He proposes a numerical solution using discrete intervals and concludes with a practical example: a non-linear dynamic analysis of a new reactor foundation for blast resistance [8].

Explosions and their effects on RC containment are a crucial area of research. Studies by Dong et al., Lin et al., and Chen et al. delve into this topic, providing valuable insights for designing safer containment vessels and storage for explosives [9, 10, 11]. Nuclear power plants in particular require RC containment structures to withstand explosive loads. Building on existing research, Pandey et al. simulated external explosions on these structures, while Hu and Lin focused on predicting failure points in specific pre-stressed concrete designs using advanced modeling techniques [12, 13]. It's important to note that studies like Keivan et al.'s, which explore the long-term effects of corrosion on RC integrity, are complementary but focus on different aspects of structural health [14].

Huang research focused on the ability of AP1000 reactor containment structures to withstand internal blast loads. They employed a simplified model, treating the internal structure as a series of rigid elements ("lumpy sticks") connected at various nodes. This model facilitated analysis of the structure's response to explosive pressures. Performance assessments for NPPs typically encompass both seismic and blast loads. This research proposes a new procedure for seismic performance assessments of NPPs. For blast loads, the focus is on the vulnerability of the containment vessel against an external terrorist bomb threat, assuming physical security measures prevent attacks within the reactor building [15]. A detailed analysis by Orenay et al. investigated how a GBU-28 bomb blast would impact a nearby AP1000 NPP containment building. Their study went beyond simple calculations and considered the complex interaction of the blast wave with soil and the resulting effect on the building structure. The model included key components like the pressure vessel, support structures, and cooling system. They used advanced techniques to precisely estimate the forces acting on critical areas. The study identified a high probability (over 1%) of failure in reactor cooling components due to a nearby GBU-28 detonation [16].

Pandey and Paul created finite element software to analyze how RC containment shells withstand explosions. Their program considers complex effects like material strain rate, cracking, and pressure under 3D loads. In simulations, a sample shell endured various explosion forces. The shell deflected the most (91.8 mm) under the faraway 0.5-ton blast, but it survived all explosions with minimal visible damage [17]. Choi et al. investigated the blast resistance of pre-stressed concrete and reinforced concrete containment structures using a combined experimental and numerical approach [18]. Asmolov et al. reviewed safety features incorporated into Russian nuclear power plants, including double containment and redundant emergency systems [19]. Jeon and Jin explored using Fiber Reinforced Concrete to improve a plant's resistance against aircraft collisions [20]. Their analysis showed significant increases in impact resistance. Armenta-Molina et al. developed a method to assess a plant's response to a subsurface explosion. Their findings suggest the structure would be safe under the simulated conditions [21].

This study investigates the response of a VVER-1200 reactor containment building (a crucial safety structure in nuclear power plants) under blast loads using computer simulations. It analyzes how the building deforms, moves, and experiences pressure under different blast scenarios. The goal is to understand how blast strength and distance affect damage and identify critical factors for improving the safety of these structures in Egyptian nuclear power plants (specifically the VVER-1200 design). This research is unique as it focuses on the VVER-1200 design, unlike previous studies on other reactor types.

2 Data Collection and Adapted methodology *case study of El -Dabaa plant*

The El-Dabaa power plant, Egypt's first NPP, is now being built in El-Dabaa city. At DNPP site, four 1,200 MWe pressurized water reactor (PWR) units were constructed, each based on

the Russian VVER-1200 (AES-2006) design. The construction of Egypt's DNPP is a huge project that will significantly alter the nation's energy environment. The El-Dabaa NPP, Egypt's first nuclear power station, is predicted to be essential in helping the nation fulfill its expanding energy needs and lessen its dependency on fossil fuels. But there are also security and safety issues with the design and maintenance of nuclear generating facilities.

2.1 Feature of the site

The DNPP site is in the ARE, on the Mediterranean coast, 135 km west of Alexandria, 5.8 km north-east of El Dabaa city center, which is part of the Governorate (Province) of Matruh, 125 km east-southeast of the city of Marsa Matruh, which is the administrative center of the province, see Figure 1-a. Situated on the northern shore, 296 kilometers (184 miles) separate it from Cairo and is connected by El-Alamein International Airport, which has been selected as the site for a new nuclear reactor. El-Dabaa also has average wind speeds (at a height of 10 m) ranging from 5 to 8 m/s throughout the year, with the winter having the highest recorded speeds (between 7.5 and 8 m/s) [22]. The reactor building, the steam cell, the auxiliary building, the safety building, and the control building are the buildings on the site, as shown in figure 1-b.

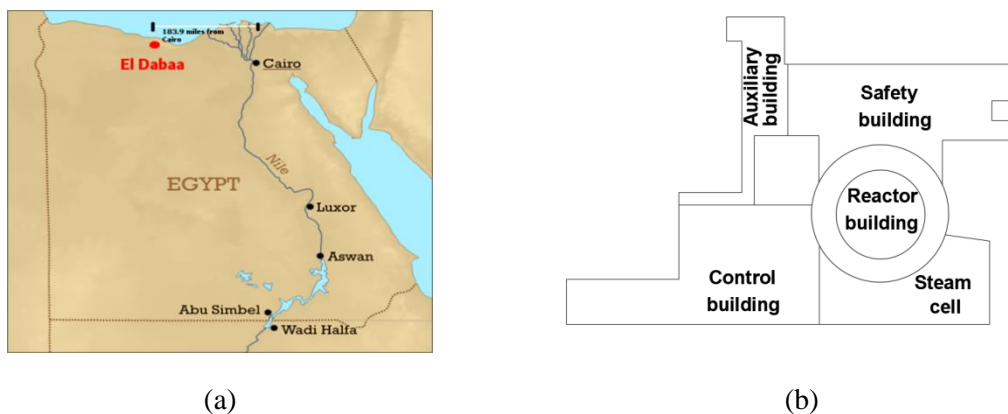


Figure 1: (a) Location of El-Dabaa site and (b) layout of El-Dabaa site.

2.2 The materials, constitutive laws and equation of state (EOS)

The behavior of the RC containment structure of the DNPP under internal and external blast loading was analyzed in this research using the finite element technique (FEM). Four materials were used in this analysis: concrete, steel, air, and explosives. Take into account the proper constitutive material models and equations of state for each material. The whole RC containment model was discretized using FEM into a limited number of smaller components. A critical aspect of this research involves identifying appropriate constitutive models and material properties that accurately represent the behavior of materials used in DNPP under various loading conditions. The material parameters and constitutive models employed in this paper are shown in Table 1 and described below [23].

Utilizing ANSYS software with explicit dynamics analysis, I performed a numerical simulation to analyze the dynamic responses of the containment under external blast loading, focusing on the damage mechanisms. The simulation considered the fluid-solid coupling interaction. Material properties were chosen from the ANSYS library. The pressure of the explosion products was modeled using the JWL EOS [24,25]. The specific JWL equation and the parameters used for TNT in ANSYS can be found below.

MAT_HIGH_EXPLOSIVE_BURN is used for explosive material. The detonation velocity of an explosive is 6930 m/s, and the JWL equation of state (EOS) can be used to simulate its behavior [24, 25, 26]

$$P = A \left(1 - \frac{\omega}{R_1 V}\right) e^{-R_1 V} + B \left(1 - \frac{\omega}{R_1 V}\right) e^{-R_2 V} + \frac{\omega E}{V} \quad (1)$$

Where V is relative volume, E is the specific internal energy of each unit of mass, A and B are linear explosion parameters, and x, R1 and R2 are nonlinear explosion parameters.

For the air the air's behavior and linear internal energy are modeled using the linear-polynomial EOS. The MieGrueisen form of the equation of state is generalized into the polynomial equation of state, which has various forms for states of tension and compression [26]. Pressure is provided by:

Regarding compression ($\mu > 0$)

$$P = A_1 \mu + A_2 \mu^2 + A_3 \mu^3 + (B_0 + B_1 \mu) \rho_0 e \quad (2)$$

Regarding Tension ($\mu < 0$)

$$P = T_1 \mu + T_2 \mu^2 + B_0 \rho_0 e \quad (3)$$

For steel, a plastic kinematic hardening model was employed to simulate the behavior of the steel reinforcement within the concrete containment structure [24]. For concrete, to simplify the analysis and reduce computational cost, we assumed elastic behavior. This is achieved by applying an isotropic elastic model [24].

Table 1: the internal explosion analysis material specifications for RC containment [23].

material	Unit Metric (m, kg, N, s, V, A) Degrees rad/s Celsius					
1- Air	Mass density = 1.225 kg/m ³ Specific heat constant pressure = 717.6 J/kg. C° *EOS_LINEAR_POLYNOMIAL					
A_1 (Pa)	A_2 (Pa)	B_0	B_1	T_1	T_2	
0	0	0.4	0.4	0	0	
2- Explosive	*MAT_HIGH_EXPLOSIVE_BURN					
Mass density (kg/m ³)	Detonation velocity (m/s)	C–J pressure (Pa)		C–J energy unit mass (KJ/Kg)		
1630	6930	2.1e10		3.681e3		
A (Pa)	B (Pa)	R_1	R_2	W		
3.7377e11	3.7471e9	4.15	0.9	0.35		
3- Steel bar	*MAT_ISOTROPIC_ELASTIC					
Mass density (kg/m ³)	shear modulus (Pa)	Poisson's ratio	Young's modulus (Pa)	bulk modulus (Pa)		
7850	7.6923e10	0.3	2.1e11	1.6667e11		
4- concrete	Mass density = 2314 kg/m ³ Specific heat constant pressure = 654 J/kg. C° *EOS_LINEAR_POLYNOMIAL					
A_1 (Pa)	A_2 (Pa)	A_2 (Pa)	B_0	B_1	T_1	T_2
3.527e10	3.958e10	9.04e9	1.22	1.22	3.527e10	0

2.3 Reinforcement containment model description

The contemporary Russian VVER-1200 reactors, such as El-Dabaa reactor, have two containment systems. Figure 2 shows the basic geometry and simulation dimensions of the VVER-1200 nuclear reactors that are the subject of this thesis. The containment building is composed of concrete shielding structures that are positioned at an elevation of +71.90 above

the ground in the form of cylindrical shapes. The outer containment physically protects the inner containment from external influences. The external shielding structure is a cylinder with an inner diameter of 50.0 m and a thickness of 2.2 m. The inner shielding structure is a cylinder with an inner diameter of 29.60 m and a thickness of 2.20 m. The foundation of the containment container is embedded in the soil at level 11.75 and is three meters thick. The mass is 1.20e8 kg and the total volume is 52622 m³.

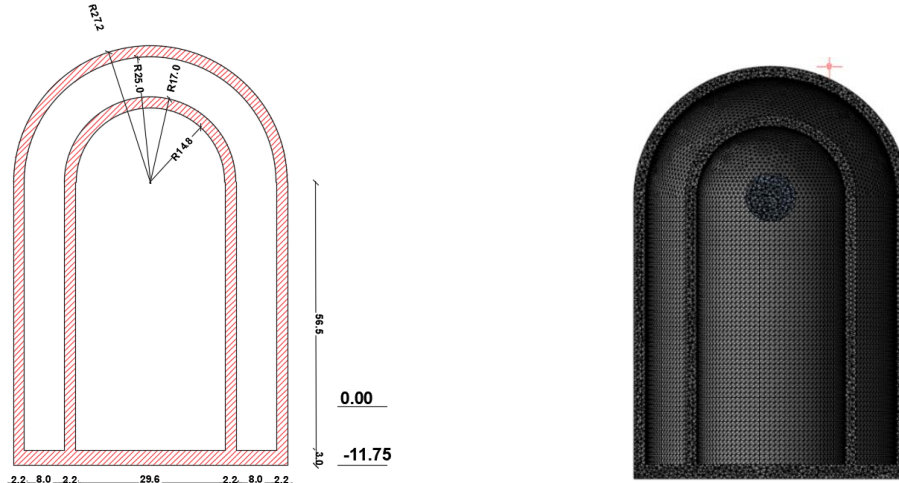


Figure 2: Reinforced containment vessel for EL-DABAA reactor building.

3 Validation

To validate my analysis of a reinforced concrete containment structure under blast loading, I compared my results with a similar study by Zhao et al. [24]. This strong agreement strengthens the validity of my own analysis, presented in detail in the following sections (including Figures 3, 4, 5). Two metrics, R-squared (R^2) and Root Mean Squared Error (RMSE), are used to compare the accuracy of a model. R^2 indicates how closely the model's predictions (extracted equivalent stress) match the reference values. It ranges from 0 to 1, with a higher value signifying a better fit. RMSE, on the other hand, measures the average difference between the model's predictions and the reference values. A lower RMSE indicates a better agreement between the model and the reference data [27].

$$R^2 = \left(\frac{n(xy) - (\Sigma x)(\Sigma y)}{\sqrt{[n\Sigma x^2 - (\Sigma x)^2]} * \sqrt{[n\Sigma y^2 - (\Sigma y)^2]}} \right)^2, \quad (4)$$

$$RMSE = \sqrt{(\Sigma(y - x)^2 / n)}, \quad (5)$$

Where x is the extracted reference equivalent stress (Pa), y is the extracted equivalent stress (Pa) and n number of points.

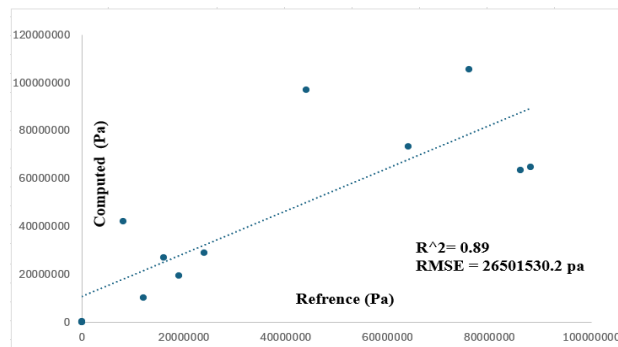


Figure 3: Relation between the reference and equivalent stress exacted.

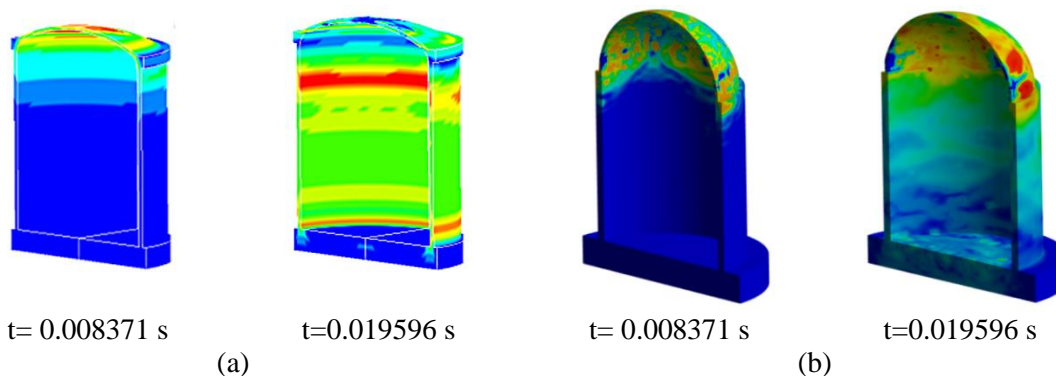


Figure 4: Von misses stress of the RC containment at scale distance of $0.778 \text{ m} / \text{Kg}^{1/3}$ for a distance 20 m (a) Extracted equivalent stress [24] and (b) Reference equivalent stress.

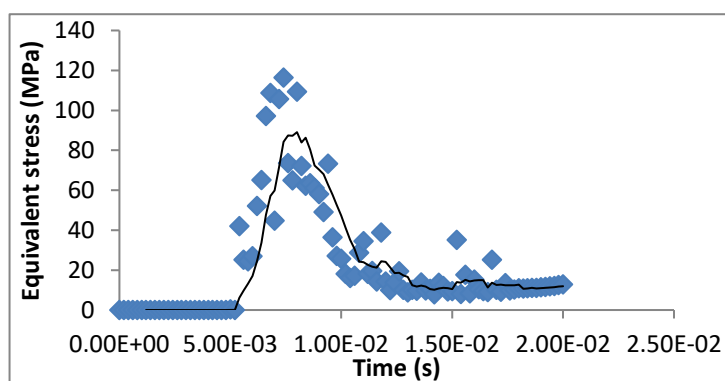


Figure 5: difference between extracted and reference equivalent stress of RC containment.

4 Damage and response of reactor structures under blast loads

Decipher the response of model reactor structures subjected to blast loads. This entails a comprehensive investigation into the effects on structural integrity, including parameters like displacement, velocity, acceleration, and pressure distribution within the structure. Additionally, the study will explore how variations in blast parameters, such as intensity and distance from the source, influence the response. An analysis was conducted to determine if the concrete containment structure of the DNPP could survive an explosive hazard emanating from four cases. Four possibilities were taken into consideration in the analysis:

Case 1: A 2,000 kg of TNT explosion that occurred inside the containment structure at a height of 56 meters and a standoff distance of 14.80 meters similar to zhao et al [24]. Case 2: To simulate the possible effects of a weapon comparable in magnitude to the one used in the Oklahoma City bombing in 1995, a 2,000 kg TNT explosion exploded 10 meters from the reactor building similar to Huang et al [15]. Case 3: Similar to Case 2, but with the containment structure elevated above the ground. Case 4: 300 kg of TNT in a high-explosive charge scenario, one meter from the outside containment similar to Ornai et al [16]. The weapon that destroyed the Murrah Federal Building in 1995 was comparable in size to the 2000 kilogram of TNT [15].

4.1 case study 1

The parameters of the blast load are taken as the charge weight = 2000 kg of TNT and the stand-off distance = 14.80 m [24]. The scaled distance = 1.175, see figure 6.

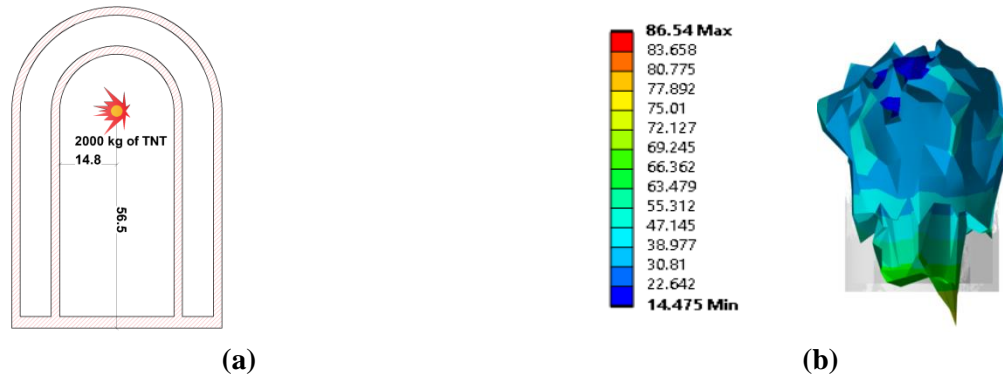


Figure 6: (a) Case study (1) and (b) displacement response of the discharge

4.2 case study 2

The parameters of the blast load are taken as the charge weight = 2000 kg of TNT, the scaled distance = 0.8 and the stand-off distance = 10.00 m [15], see figure 7. Additionally, we modelled the interaction between the blast wave and soil, as well as the subsequent interaction between the soil and the containment structure, following a similar approach to Ornai et al. [16]. This differs from the empirical formula-based method used in Huang and Whittaker's study [15].

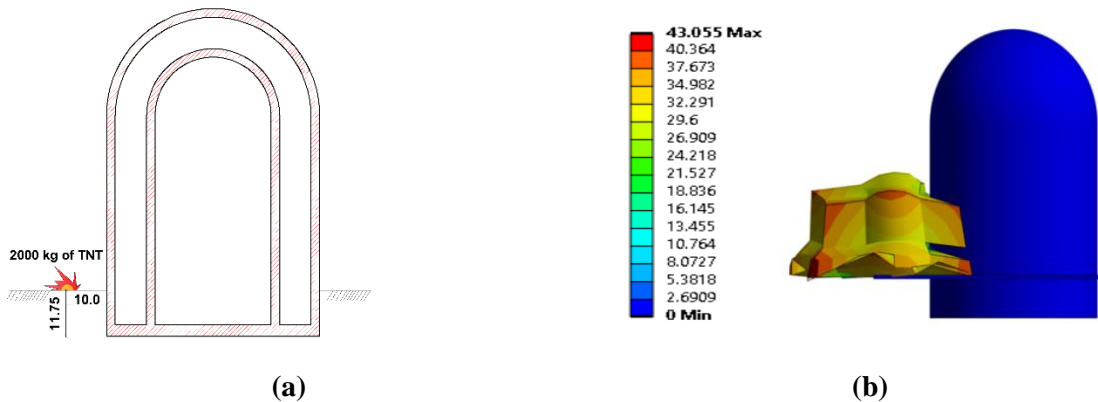


Figure 7: (a) Case study (2) and (b) displacement response of the discharge

4.3 case study 3

The parameters of the blast load are taken as the charge weight = 2000 kg of TNT, the scaled distance = 0.8 and the stand-off distance = 10.00 m [15].

The current analysis assumes a ground-based containment building, differing from the actual Dabaa configuration. This specific case and the on-going Dabaa study are not directly related and intended for separate investigations. Our objective lies in contrasting the response of the concrete containment building, particularly its behaviour when located below the ground surface, with the findings presented in the third case study. By analysing containment building behaviour under diverse scenarios, we aim to contribute valuable insights for future design and safety assessments, see figure 8.

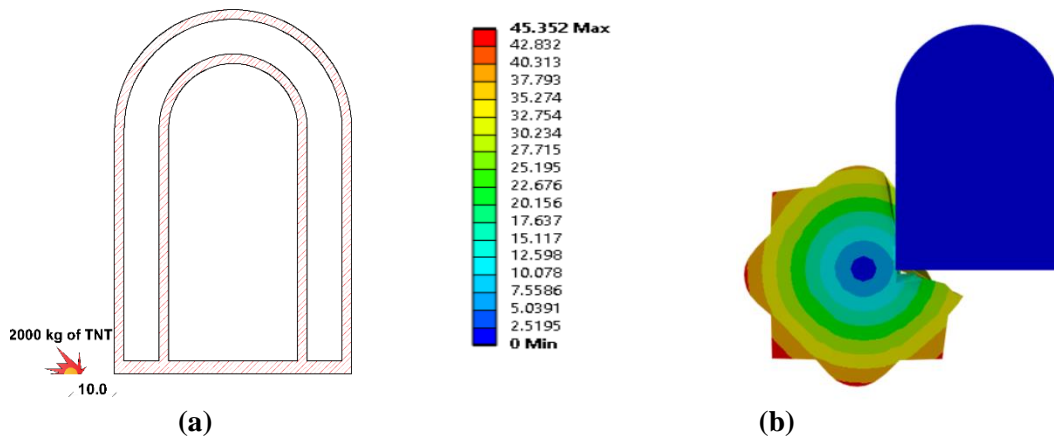


Figure 8: (a) Case study (2) and (b) displacement response of the discharge.

4.4 case study 4

The parameters of the blast load are taken as the charge weight = 300 kg of TNT, the scaled distance = 0.15 and the stand-off distance = 1.00 m see figure 9.

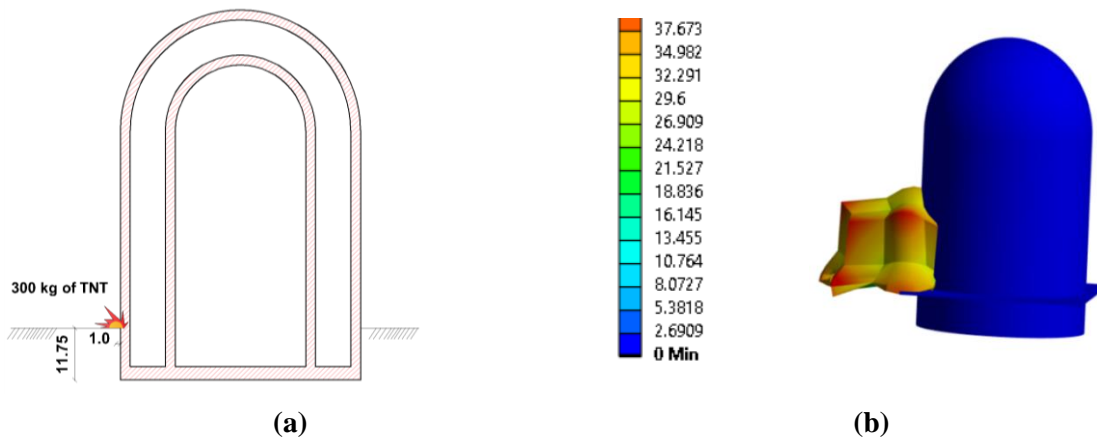


Figure 9: (a) Case study (4) and (b) displacement response of the discharge

5 Numerical results and discussion

The numerical results of the parametric study carried out in this section for the response of RC containment structure are shown in figures (10) to (23) and tables (2) to (3) by using ANSYS program. Based on an extensive investigation of the numerical results obtained, the following remarks are drawn:

- 1- The purpose of case 1 is to do an initial assessment of the acceleration forces caused by a possible danger to facilitate the examination of several LOCA scenarios. This case centers on the containment structure made of reinforced concrete, whose collapse has been linked to several accidents in the past. Figures 10–11 most likely show maps of pressure and displacement for the structure at various times throughout the blast.

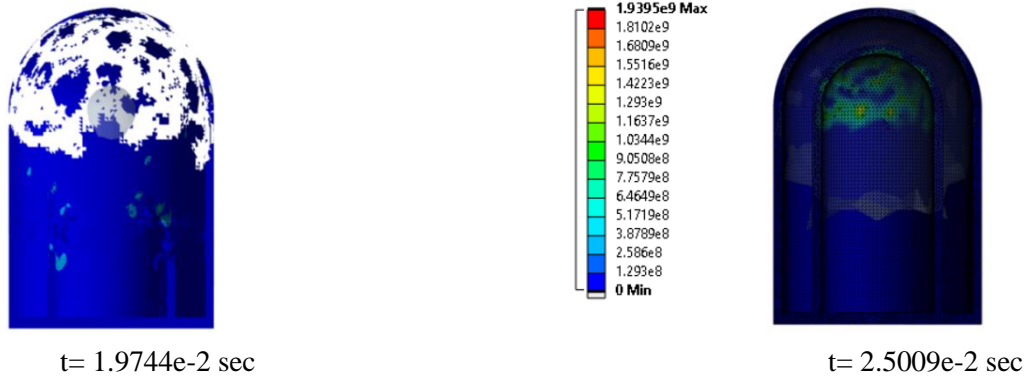


Figure 10: variation of pressure with time.

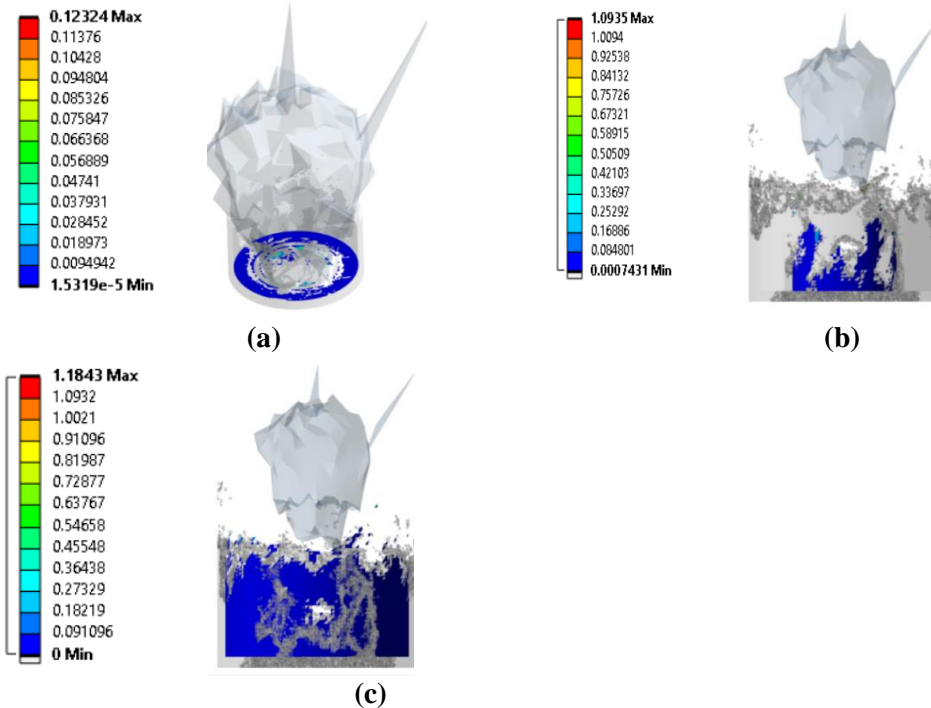


Figure 11: (a) displacement response of the base, (b) displacement response of the inner containment and (c) displacement response of the outer containment.

2- Also for case 1, Figure 12 presents the analytical results and shows the calculated pressure distribution induced by the internal explosion inside the structure. The graphic effectively depicts the shock wave traveling through the structure and rising above 86.54 meters at various points in time from the base. Figure 15 makes it clear that the first impact of the strong pressure wave may have made the dome the weakest point. This prompted worries about the possibility of a dome failure during an internal gas explosion, akin to the March 11, 2011, event at the Fukushima nuclear power plant. For this reason, it is essential to reinforce the RC containment dome while designing and building nuclear power facilities. The study discovered a maximum displacement of about 1.18 meters that happened at 0.25 milliseconds. The pressure in the blast wave peaked at 0.112 milliseconds, or roughly 1939.50 MPa in air, which is not too far from ambient pressure. The greatest velocity was about 861.32 m/s at 0.25 milliseconds (Figure 12). In the end, the maximum acceleration components were about 2.01 m/ms² at 0.112 milliseconds.

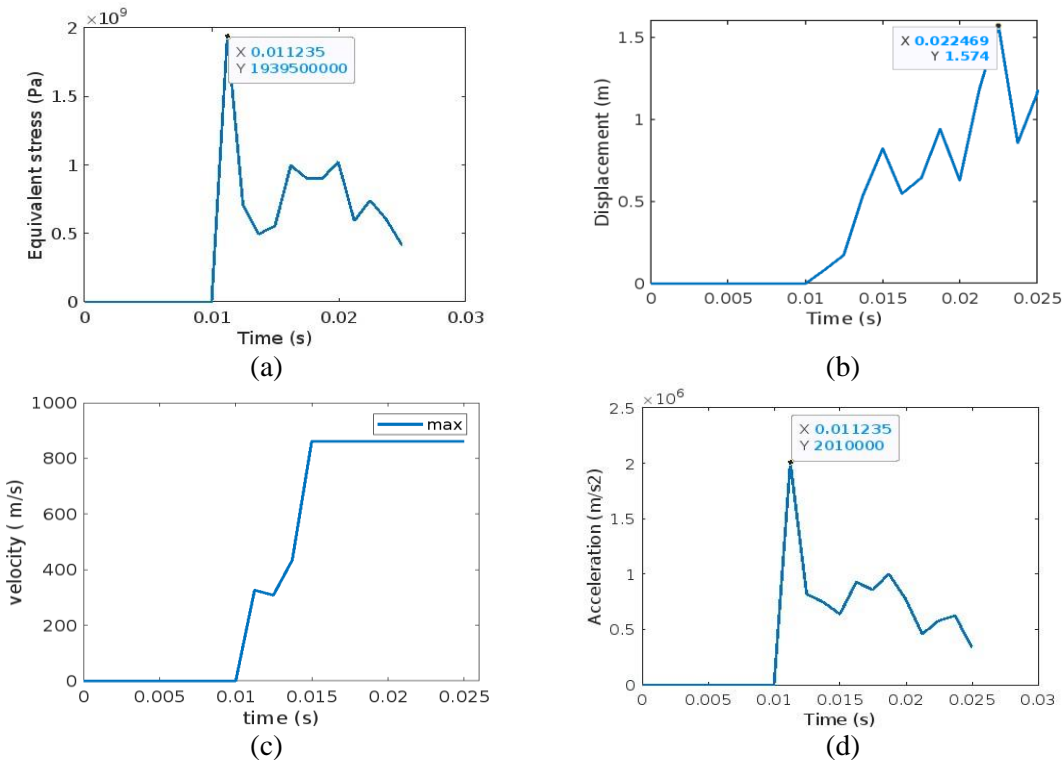


Figure 12: Response of RC containment, (a) Equivalent stress, (b) Displacement response of containment, (c) Velocity response and (d) Acceleration response.

3- CASE 2, Maps of pressure and displacement for the structure at different points during the blast are probably depicted in Figures 13 –14. A maximum displacement of roughly 0.74 millimeters, occurring at 6.3 milliseconds, was found by the research. At 3.15 milliseconds, the pressure in the blast wave peaked at approximately 6.41 MPa in air, which is close to ambient pressure. At 9 milliseconds, the maximum velocity was approximately 4904.3 m/s (Figure 14). Ultimately, at roughly 3.15 milliseconds, the peak acceleration components were on the order of 177.6 m/ms².

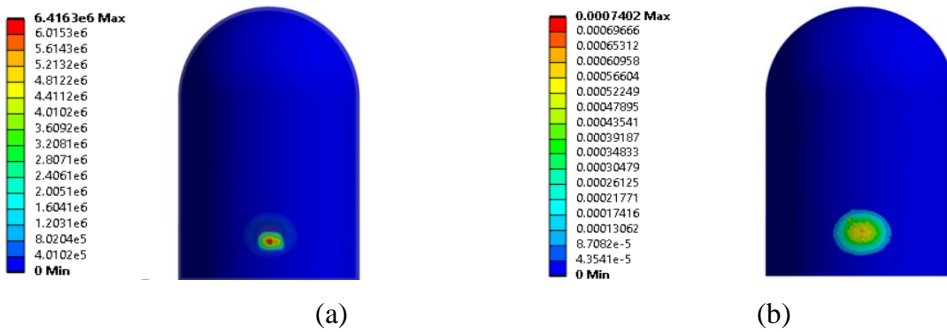


Figure 13: (a) pressure destruction inside the RC containment, (b) the displacement response of outer containment.

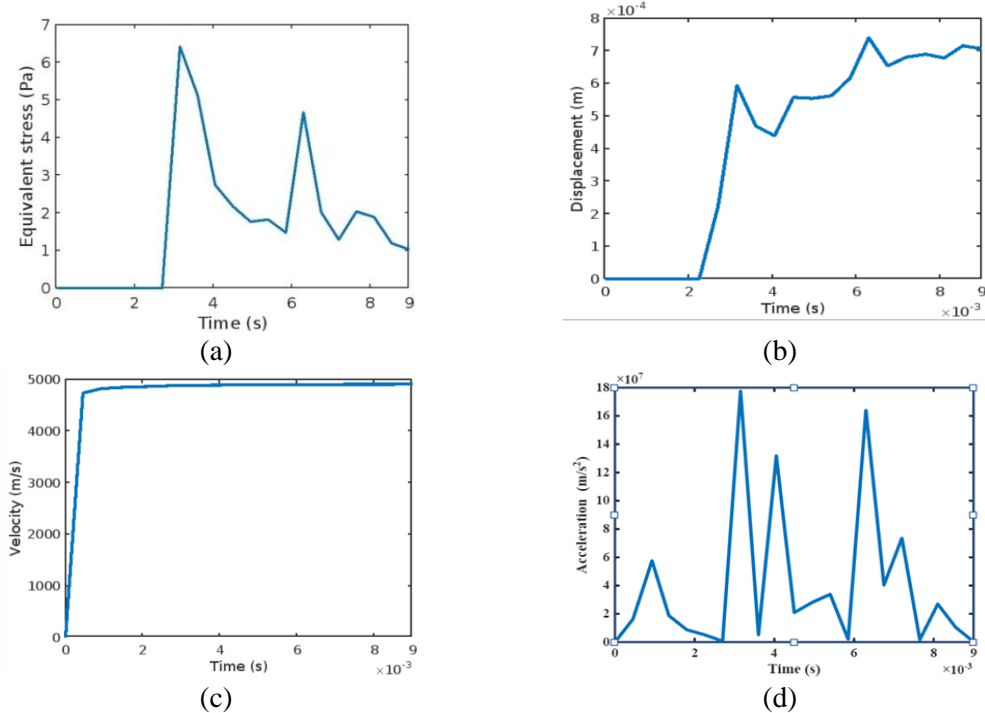


Figure 14: Response of RC containment, (a) Equivalent stress, (b) Displacement response of containment, (c) Velocity response and (d) Acceleration response.

4- CASE 3, Maps of pressure and displacement for the structure at different points during the blast are probably depicted in Figures 15–16-17. A maximum displacement of roughly 1.10 millimeters, occurring at 7.65 milliseconds, was found by the research. At 3.15 milliseconds, the pressure in the blast wave peaked at approximately 13.225 MPa in air, which is close to ambient pressure. At 2.7 milliseconds, the maximum velocity was approximately 2.234 m/s. Ultimately, at roughly 8.55 milliseconds, the peak acceleration components were on the order of 0.14 m/ms². ecipher the response of model reactor structures subjected to blast loads. This entails a comprehensive.

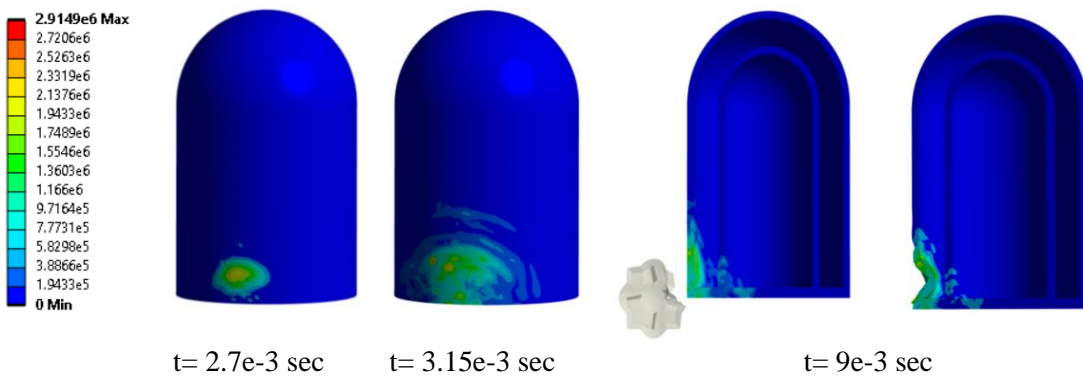


Figure 15: Variation of pressure with time

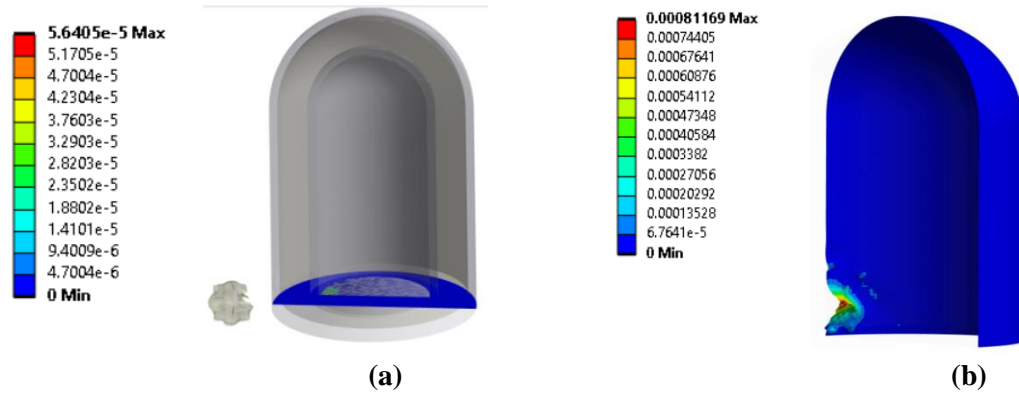


Figure 16: (a) displacement response of the base and (b) displacement response of the outer containment.

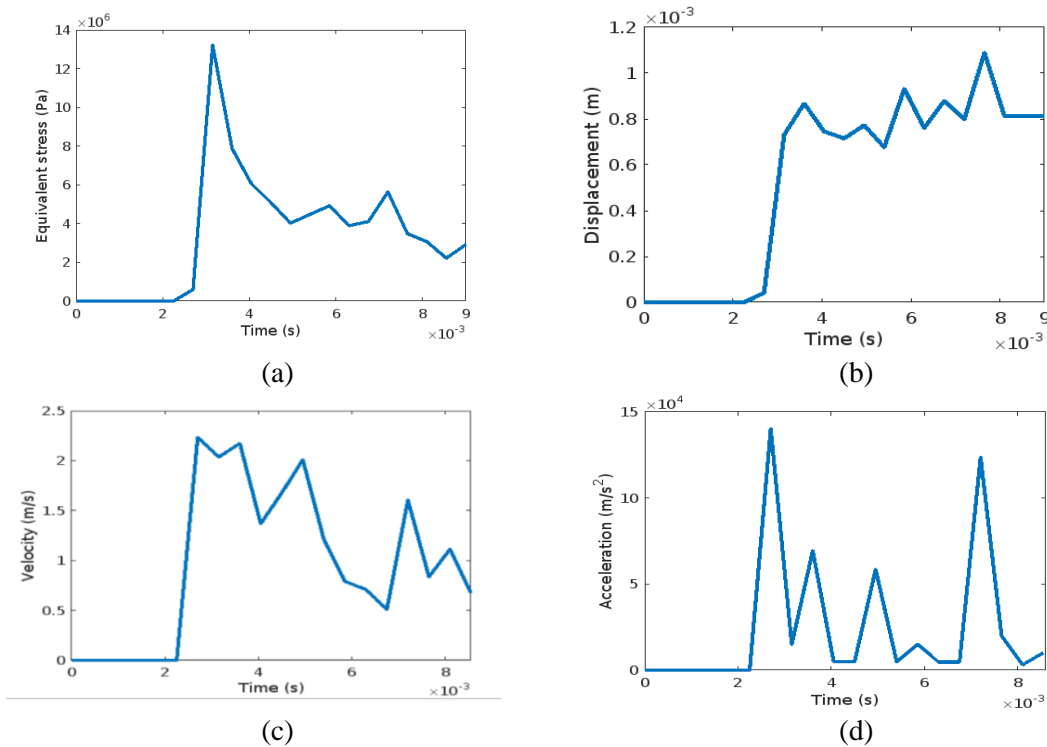
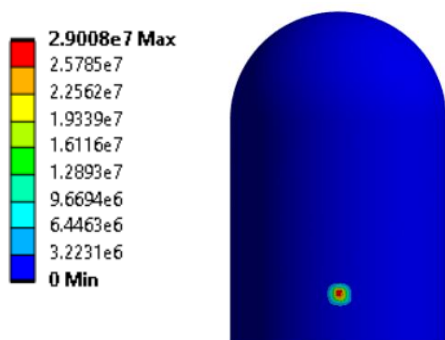


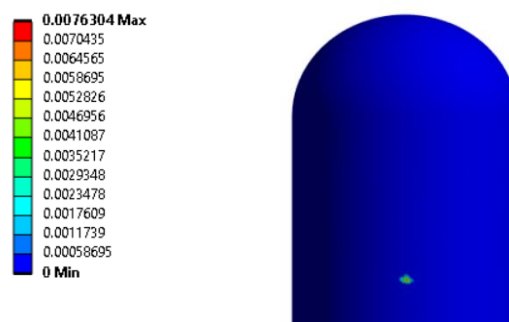
Figure 17: Response of SDOF system, (a) Equivalent stress, (b) Displacement response, (c) Velocity response and (d) Acceleration response.

5- CASE 4, the FEM was used to simulate the interaction between the blast wave and the structure by a particular coupling technique. This method simulates the pressure field created by the explosion and how it interacts with the structural elements. The parameters of the blast load are taken as the charge weight = 300 kg of TNT, the scaled distance = 0.15 and the stand-off distance = 1.00 m. Maps of pressure and displacement for the structure at different points during the blast are probably depicted in Figures 18 to 20. A maximum displacement of roughly 7.04 millimeters, occurring at 0.903 milliseconds, was found by the research. At 0.9 milliseconds, the pressure in the blast wave peaked at approximately 33.3 MPa in air, which is close to ambient pressure. At 0.903 milliseconds, the maximum velocity was approximately 4255.2 m/s (Figure 19). Ultimately, at roughly 0.452 milliseconds, the peak acceleration components were on the order of $8.47 \times 10^7 \text{ m/s}^2$.



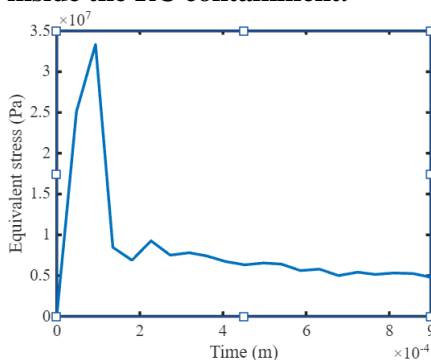
(b) $t=9.0305 \times 10^{-4}$ sec

Figure 18: pressure destruction inside the RC containment.

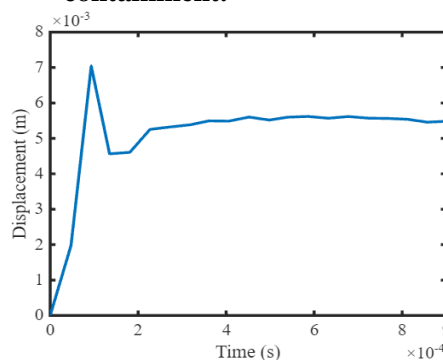


(a)

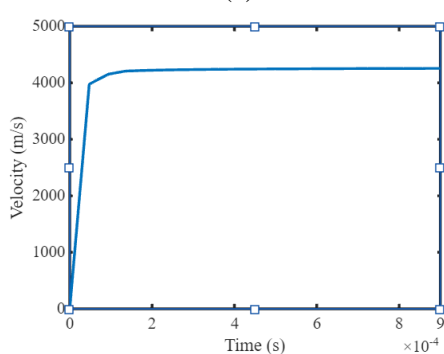
Figure 19: displacement response of outer containment.



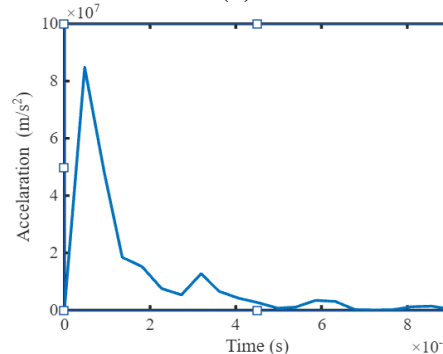
(a)



(b)



(c)



(d)

Figure 20: Response of RC containment, (a) Equivalent stress, (b) Displacement response of containment, (c) Velocity response and (d) Acceleration response.

6- Comparing the second and third cases, the displacement of the inner wall of the concrete containment building for the nuclear reactor is significantly reduced when placed underground. In Case 3, the displacement is 0.042 mm, while in Case 2, it is only 0.00222 mm, representing a substantial decrease. Similarly, the displacement of the outer wall exhibits a noticeable reduction, dropping from 0.82 mm in Case 3 to 0.74 mm in Case 2, a decrease of 9.66%. Furthermore, the distance traveled by blast fragments decrease from 45.35 meters in Case 3 to 43.055 meters in Case 2. Additionally, the pressure level is higher in Case 3 (13.22 MPa) compared to Case 2 (6.41 MPa). These findings demonstrate that lowering the containment building's position relative to the ground surface significantly reduces the impact of explosions on the structure (figure 21). This is due to the soil acts as a shock absorber, dissipating the blast wave's energy, and its load-bearing capacity distributes the pressure over a wider area, reducing structural stress.

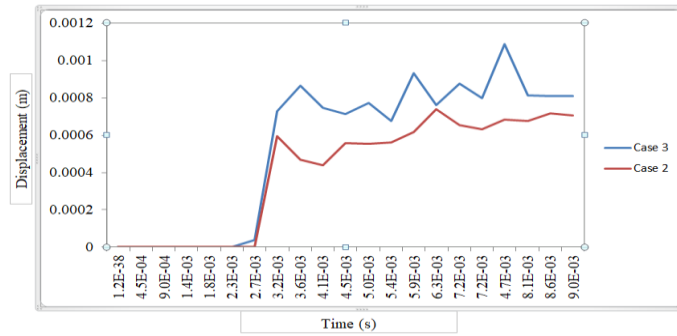
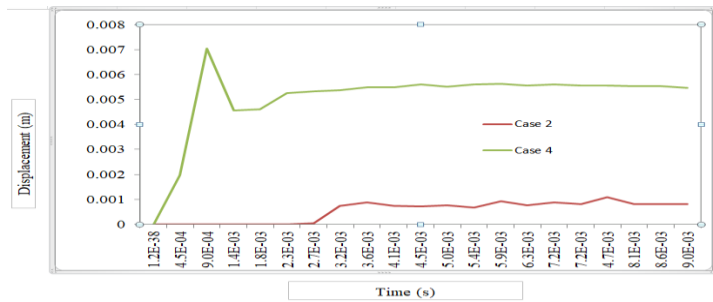
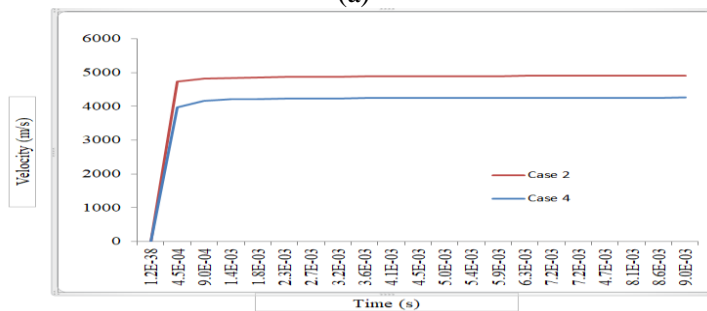


Figure 21: the difference between the displacement in case study (2) and case study (3)

7- Cases 2 and 4 investigate the effect of a reduced explosive charge and closer proximity to the containment building. In these cases, the charge is lowered from 1000 kg of TNT to 300 kg of TNT, and the facing distance is reduced from 10 meters to 1 meter. Interestingly, despite the decrease in charge size (70% reduction), the response of the containment building in Case 4 exhibit a significant increase compared to Case 2. The displacement of the structure in Case 4 increases by a factor of approximately 10, from 0.74 mm to 7.69 mm. This observation highlights the importance of considering proximity effects in blast analysis. While the total energy released by the explosive is reduced, the closer proximity of the charge in Case 4 leads to a more concentrated load on the structure, resulting in a larger displacement. However, the equivalent stress for the structure in Case 4 exhibits a decrease compared to Case 2. The equivalent stress value drops from 2.90×10^7 Pa to 6.42×10^6 Pa, representing a decrease of approximately 77.8%. This suggests that while the displacement increases due to the closer proximity, the overall stress state within the structure remains below a critical failure point. An analysis of the velocity revealed a decrease in Case 4 compared to Case 2. The velocity in Case 4 was measured at 4798.7 m/s, representing a reduction of 2.2% from the velocity observed in Case 2 (4904.3 m/s) (figure 22).



(a)



(b)

Figure 22: the difference between the (a) displacement in case study (2) and case study (4) and (b) velocity between the same cases.

8- The dual containment system, consisting of an inner and outer concrete enclosure, provides a robust defense against potential accidents. To illustrate its effectiveness, we can analyze the displacement reductions observed in simulated accident scenarios: Case 2, the inner containment significantly reduces its displacement, reaching a mere 0.0022 millimeters. This substantial reduction (compared to the outer containment's 0.7402 mm displacement, representing a 99% difference) highlights its ability to absorb the initial impact. Case 3, Similar to Case 2, the inner containment effectively mitigates displacement, going from 0.812 millimeters to a minimal 0.042 millimeters (a 95% reduction). Case 4, the inner containment demonstrates its effectiveness once more, with a minimal displacement reduction (0.032 millimeters) compared to the significant initial displacement of the outer containment (7.63 millimeters), see figure 23.

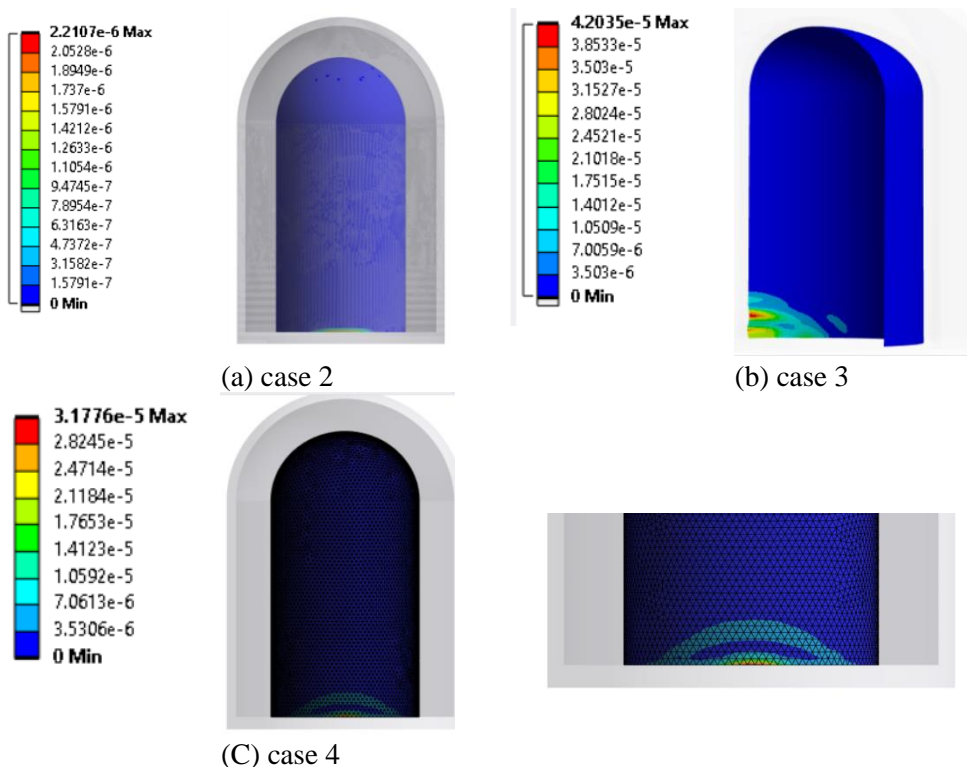


Figure 23: displacement response of inner containment for different cases.

6 Vulnerability assessments of nuclear power plants to explosions

This section outlines the key principles of vulnerability associated with external explosions impacting a NPP. These principles are crucial for understanding potential risks and conducting a comprehensive explosion assessment. The analysis considers two main scenarios:

- 1- Aircraft Crash: An aircraft crash represents a potential external threat to an NPP. Studies have identified the dome as a vulnerable point due to its proximity to the source of the explosion and the initial pressure impact. Additionally, the complex pressure wave propagation within the containment structure due to reflections differs from a free-field explosion, requiring careful consideration. Understanding the specific failure modes of the dome and the effectiveness of existing safety systems in evacuating personnel, limiting radioactive material spread, and protecting the environment is crucial.
- 2- External Blast (Bomb): A bomb detonated near the NPP presents another external threat. Here, the focus shifts to the containment structure's ability to withstand the blast and fragments:

Primary Containment Breach: A critical vulnerability lies in the potential breaching or perforation of the outer shielding structure due to the blast and fragments. As indicated in [29], close proximity hits (up to 1 meter) pose a significant risk and would necessitate immediate NPP shutdown for repairs. This highlights the importance of the double containment structure, a key feature in modern Russian reactors, for mitigating the impact of explosions and shrapnel.

Internal Shock and Equipment Failure: The blast and fragments can generate an in-structure shock wave that may exceed the shock tolerance of critical engineering systems and equipment within the NPP. This raises the possibility of internal failures, such as a pressurizer or safety system malfunction, leading to a LOCA and potentially a core meltdown with subsequent radioactive release. Shock tolerance values are established based on the specific demands of nuclear reactors, as outlined by the Nuclear Energy Institute [29].

Vulnerability of Control Room and Other Facilities: An investigation into the vulnerability of other critical NPP facilities, such as the control room, is essential. Failures in these areas could also trigger LOCA or other catastrophic events [30].

7 Conclusions

This study investigates the damage mechanisms and dynamic response of a RC containment structure subjected to an internal blast using ANSYS, a non-linear dynamic finite element analysis program.

1. The vulnerability of structures subjected to blast loads is demonstrably influenced by two key parameters: the explosive charge weight and the stand-off distance between the explosion and the target. This underscores the paramount importance of maximizing the stand-off distance in blast mitigation strategies. By strategically increasing the separation between a potential explosion and surrounding buildings, engineers can significantly reduce the damaging effects of the blast and enhance the overall resilience of the structures.
2. These results demonstrate that lowering the containment building's position relative to the ground surface significantly mitigates the impact of explosions on the structure, leading to a reduced response. This compelling evidence underscores the need for further research into the viability of establishing nuclear power reactors underground.
3. This paper explores safety standards for explosion prevention and protection in nuclear power plants. The focus is on implementing rational measures based on the concept of system safety. These measures aim to prevent explosions in the first place and mitigate their impact if they do occur. By adhering to these standards and fostering a culture of preparedness, the author emphasizes the importance of achieving robust explosion prevention and protection at nuclear facilities.
4. Comprehensive assessments of potential accidents, including explosions originating from within or outside the DNPP, highlight the critical need for robust safety protocols and effective interventions. This proactive approach allows Egypt to strengthen its nuclear safety framework, emergency response capabilities, and adherence to international safety standards. By addressing these worst-case scenarios upfront, Egypt fosters public trust and ensures the long-term sustainability of its nuclear energy program.

8 Future researches

The research on the integration of nuclear power can be expanded to cover more topics, even though my thesis concentrates on the specific response of reinforced containment structures under blast loads. The following are possible areas for further research:

1. Expanding the research scope to encompass nuclear safety in Egypt can be achieved by delving into two critical aspects: assessing nuclear safety in the face of explosions and examining nuclear waste management practices.
2. A comprehensive vulnerability assessment of the entire NPP site, including surrounding buildings, should be considered.
3. Underground nuclear power plants deserve a closer look! Future research should weigh their potential safety and environmental benefits against the construction and operational challenges. This could lead to a safer, cleaner, and more publicly accepted way to produce nuclear energy.
4. Expanding this effort to include connecting nuclear energy to wind turbines. It is possible to improve energy production, sustainability, and grid stability by strategically integrating nuclear power with wind energy, two different but promising sources of electricity generation.
5. An investigation of the combination of nuclear power and seawater desalination would greatly broaden the scope of our thesis. By addressing water scarcity and diversifying energy sources, this offers an excellent chance to address two pressing global issues and provide a long-term solution.

18. Choi, J. H., Choi, S. J., Kim, J. H. J., & Hong, K. N. (2018). Evaluation of blast resistance and failure behavior of prestressed concrete under blast loading. *Construction and Building Materials*, 173, 550-572.
19. Asmolov, V. G., Gusev, I. N., Kazanskiy, V. R., Povarov, V. P., & Statsura, D. B. (2017). New generation first-of-the-kind unit–VVER-1200 design features. *Nuclear Energy and Technology*, 3(4), 260-269.
20. Jeon, S. J., & Jin, B. M. (2016). Improvement of impact-resistance of a nuclear containment building using fiber reinforced concrete. *Nuclear Engineering and Design*, 304, 139-150.
21. Armenta-Molina, A., Villanueva-García, A., Soto-Mendoza, G., Pérez-Montejo, S., Ruiz-López, P., Beltrán-Fernández, J. A., & Urriolagoitia-Calderón, G. M. (2020). Structural Vibrations in a Building of a Nuclear Power Plant Caused by an Underground Blasting. *Engineering Design Applications III: Structures, Materials and Processes*, 81-90.
22. ElShafeey, N., Eid, M. M., Mahmoud, A. S., & Zakey, A. S. (2023). Risk Assessment of Possible Hazards of El Dabaa Nuclear Power Plant Using FLEXPART Model. *Engineering Proceedings*, 31(1), 86.
23. Pi, S. J., Cheng, D. S., Cheng, H. L., Li, W. C., & Hung, C. W. (2012). Fluid–structure-interaction for a steel plate subjected to non-contact explosion. *Theoretical and Applied Fracture Mechanics*, 59(1), 1-7.
24. Zhao, C. F., Chen, J. Y., Wang, Y., & Lu, S. J. (2012). Damage mechanism and response of reinforced concrete containment structure under internal blast loading. *Theoretical and Applied Fracture Mechanics*, 61, 12-20.
25. Dobratz, B. M. (1981). *Explosive Handbook*. UCRL-52997, Lawrence Livermore National Laboratory. Livermore, CA.
26. Jha, N., & Kumar, B. K. (2014). Under water explosion pressure prediction and validation using ANSYS/AUTODYN. *Int. J. Sci. Res*, 3(12), 1162-1166.
27. Sinnamon, R. M., & Andrews, J. D. (1996, January). Fault tree analysis and binary decision diagrams. In *Proceedings of 1996 Annual Reliability and Maintainability Symposium* (pp. 215-222). IEEE.
28. Chicco, D., Warrens, M. J., & Jurman, G. (2021). The coefficient of determination R-squared is more informative than SMAPE, MAE, MAPE, MSE and RMSE in regression analysis evaluation. *Peerj computer science*, 7, e623.
29. NEI, U. (2011). *Methodology for performing aircraft impact assessments for new plant designs*. NEI 07-13 Revision 8P.
30. Brandys, I., Ornai, D., & Ronen, Y. (2017). Integrated blast resistance model of nuclear power plant auxiliary facilities. *Journal of Nuclear Engineering and Radiation Science*, 3(3), 030903.